The Journal of Immunology

Functional Attributes of Antibodies, Effector Cells, and Target Cells Affecting NK Cell – Mediated Antibody-Dependent Cellular Cytotoxicity

A. Robin Temming, Steven W. de Taeye, Erik L. de Graaf, Louise A. de Neef, Gillian Dekkers, Christine W. Bruggeman, Jana Koers, Peter Ligthart, Sietse Q. Nagelkerke, James C. Zimring, Taco W. Kuijpers, Manfred Wuhrer, Theo Rispens and Gestur Vidarsson

J Immunol 2019; 203:3126-3135; Prepublished online 20 November 2019;
doi: 10.4049/jimmunol.1900985
http://www.jimmunol.org/content/203/12/3126

The Journal of Immunology is published twice each month by
The American Association of Immunologists, Inc.,
1451 Rockville Pike, Suite 650, Rockville, MD 20852

Print ISSN: 0022-1767 Online ISSN: 1550-6606.

Functional Attributes of Antibodies, Effector Cells, and Target Cells Affecting NK Cell–Mediated Antibody-Dependent Cellular Cytotoxicity

A. Robin Temming,*,[1] Steven W. de Taeye,*,†,[1] Erik L. de Graaf,* Louise A. de Neef,‡ Gillian Dekkers,† Christine W. Bruggeman,§ Jana Koers,† Peter Ligthart,¶ Sietse Q. Nagelkerke,§,‖ James C. Zimring,# Taco W. Kuijpers,§,‖ Manfred Wuhrer,‡ Theo Rispens,† and Gestur Vidarsson*

Ab-dependent cellular cytotoxicity (ADCC) is one of the most important effector mechanisms of tumor-targeting Abs in current immunotherapies. In ADCC and other Ab-dependent activation of myeloid effector cells, close cell–cell contact (between effector and target cell) and formation of immunological synapses are required. However, we still lack basic knowledge on the principal factors influencing ADCC potential by therapeutic Abs. In this study we investigated the combined roles of five factors affecting human NK cell–mediated ADCC, namely: 1) Ag density, 2) target cell membrane composition, 3) IgG FcγR polymorphism, 4) FcγR-blocking cytophilic Abs, and 5) Ab fucosylation. We demonstrate that the magnitude of NK cell–mediated ADCC responses is predominantly influenced by Ag density and Ab fucosylation. Afucosylation consistently induced efficient ADCC, even at very low Ag density, where fucosylated target Abs did not elicit ADCC. On the side of the effector cell, the FcγRIIIa–Val/Phe158 polymorphism influenced ADCC potency, with NK cells expressing the Val158 variant showing more potent ADCC. In addition, we identified the sialic acid content of the target cell membrane as an important inhibitory factor for ADCC. Furthermore, we found that the presence and glycosylation status of aspecific endogenous Abs bound to NK cell FcγRIIIa (cytophilic Abs) determine the blocking effect on ADCC. These five parameters affect the potency of Abs in vitro and should be further tested as predictors of in vivo capacity. ***The Journal of Immunology*****, 2019, 203: 3126–3135.**

Antibodies form a first line of defense in the adaptive immune system against infectious agents. IgG Abs are particularly important because of their long half-life and versatile effector functions, inducing both complement activation and Ig FcγR-mediated effector functions. This includes phagocytosis and Ab-dependent cellular cytotoxicity (ADCC), the latter of which is particularly important for warding off virally infected cells but also for therapeutic Ab applications in cancer treatment. However, ADCC is also an important feature in some Ab-mediated pathologies, such as the hemolytic diseases of the fetus and newborn, in which maternal IgG Abs form against paternal Ags on RBCs of the fetus, causing severe and, sometimes, life-threatening anemia (1, 2).

To improve the efficacy of mAb therapies, Ab engineering is used, and many ingenious ways have been discovered that enhance its functions (3). This includes engineering of both the protein backbone and the attached glycans. Mammalian IgG contain a highly conserved *N*-linked glycosylation site in the Fc portion that is essential for its effector functions, both for FcγR and complement component C1q binding (4–7). This glycan attached to the

*Department of Experimental Immunohematology, Sanquin Research and Landsteiner Laboratory, Amsterdam University Medical Center, University of Amsterdam, 1066 CX Amsterdam, the Netherlands; †Department of Immunopathology, Sanquin Research and Landsteiner Laboratory, Amsterdam University Medical Center, University of Amsterdam, 1066 CX Amsterdam, the Netherlands; ‡Center for Proteomics and Metabolomics, Leiden University Medical Center, 2333 ZA Leiden, the Netherlands; §Department of Blood Cell Research, Sanquin Research and Landsteiner Laboratory, Amsterdam University Medical Center, University of Amsterdam, 1066 CX Amsterdam, the Netherlands; ¶Erythrocyte Serology, Sanquin, 1066 CX Amsterdam, the Netherlands; ‖Department of Pediatric Immunology and Infectious diseases, Emma Children's Hospital, Amsterdam University Medical Center, University of Amsterdam, 1105 AZ Amsterdam, the Netherlands; and #Department of Pathology, Carter Immunology Center, University of Virginia School of Medicine, Charlottesville, VA 22903

[1]A.R.T. and S.W.d.T. contributed equally and share first authorship.

ORCIDs: 0000-0002-4104-0522 (A.R.T.); 0000-0001-7915-9230 (S.W.d.T.); 0000-0002-2208-831X (E.L.d.G.); 0000-0001-7001-0683 (L.A.d.N.); 0000-0002-9127-356X (G.D.); 0000-0001-8359-4016 (S.Q.N.); 0000-0001-5621-003X (G.V.).

Received for publication August 14, 2019. Accepted for publication October 4, 2019.

This work was supported by Genmab and Landsteiner Foundation for Blood Transfusion Research Grant 1527.

A.R.T. and S.W.d.T. performed and designed the Ab-dependent cellular cytotoxicity assays and isolated and cultured effector cells. G.D. cloned and produced the expression vectors encoding human anti-Rhesus D (RhD), anti-K, and anti-2,4,6-trinitrophenol (TNP) IgG1. S.W.d.T. and G.D. glycoengineered, produced, and isolated the human anti-RhD and anti-TNP IgG1. A.R.T. performed the flow cytometry experiments. L.A.d.N. performed mass spectrometry IgG glycosylation analyses of plasma and eluted Abs, which were supervised by M.W. E.L.d.G. performed data analysis of the IgG glycosylation. E.L.d.G. and L.A.d.N. wrote the IgG glycosylation analysis part of the *Materials and Methods* section. J.C.Z. provided the anti-K Abs. J.K. provided *Sambucus nigra* agglutinin (SNA) and neuraminidase and conjugated Alexa Fluor 405 to SNA. P.L. provided the RhD- and K-expressing RBC target cells and genotyping information, supervised the bromelain treatment, and wrote the bromelain treatment sentence in the *Materials and Methods*. S.Q.N., T.W.K., and C.W.B. performed and/or provided information about donor-specific *FCGR3A* genotyping. G.V. and T.R. designed experiments and supervised the project. A.R.T., S.W.d.T., T.R., and G.V. wrote the manuscript, which was critically reviewed by all authors.

Address correspondence and reprint requests to Dr. Gestur Vidarsson, Department of Experimental Immunohematology, Sanquin Research and Landsteiner Laboratory, Amsterdam University Medical Center, University of Amsterdam, Plesmanlaan 125, 1066 CX Amsterdam, the Netherlands. E-mail address: g.vidarsson@sanquin.nl

The online version of this article contains supplemental material.

Abbreviations used in this article: ADCC, Ab-dependent cellular cytotoxicity; gMFI, geometric mean fluorescent intensity; GPA, glycophorin A; RhD, Rhesus D; SIGLEC, sialic acid–binding Ig-type lectin; TNP, 2,4,6-trinitrophenol.

asparagine residue (Asn) at position 297 has a biantennary structure with a core consisting of mannose and *N*-acetylglucosamine residues, which can be variably extended with other sugar moieties, including galactose, sialic acid, *N*-acetylglucosamine, and fucose. Subtle changes in the composition of the Asn297 glycan influence the binding affinity of IgG for FcγRs, thereby fine-tuning the magnitude of effector functions initiated, including ADCC and Ab-dependent cellular phagocytosis (1, 4, 5, 8–10).

It has become apparent in recent years that Ab responses in humans against alloantigens (1, 11, 12) and some viral proteins (13, 14) show signs of lowered fucosylation that enhance their ADCC potential. This is particularly striking, as human IgG Fc glycans are normally highly fucosylated (~94%) (4, 15), and afucosylation of the Asn297 glycan increases the affinity for FcγRIIIa (CD16a), which improves Fc-triggered effector functions (1, 4, 8, 16–18). Because of these characteristics, it is not surprising that glycoengineering tools aiming at lowering Fc fucosylation (hypofucosylation) are already applied to increase the potency of therapeutic Abs in cancer immunotherapies (16, 19, 20).

Fucosylated antitumor Abs trigger, in general, weaker NK cell–mediated ADCC of target cells (20). Unlike hypofucosylated IgG, fucosylated Abs are sometimes not capable of triggering NK cell–mediated ADCC (4, 8, 21). Surprisingly, even relatively high concentrations of the fucosylated Ab were found to be insufficient to induce killing (4, 21, 22). The effect of IgG afucosylation on ADCC magnitude by NK cells may be dependent on the Ag and, in particular, the density of the target Ag, the nature of the Ag itself, as well as the structural orientation of the epitope on the Ag. The composition of the target cell membrane, on which the Ag is displayed, is another factor that might influence ADCC. RBCs, for example, have a thick sialic acid–containing glycan layer, termed glycocalyx, giving these cells a negative charge known as the ζ-potential. On the side of the effector cell, a confounding factor for ADCC efficiency is an FcγRIIIa polymorphism. The high-affinity FcγRIIIa with a valine residue at position 158 (Val158) and low-affinity FcγRIIIa–phenylalanine 158 (Phe158) variants, have been described to have 2–5-fold difference in affinity for fucosylated IgG1 (4, 8, 23).

Inspired by the puzzling findings that fucosylated Abs sometimes have no apparent effector function, whereas identical hypofucosylated IgG often induce strong ADCC, we dissected various parameters affecting NK cell–mediated ADCC efficiency on both the effector and target cell side. This included FcγRIIIa polymorphism, nature of the Ag, glycocalyx composition, and cytophilic Abs (aspecific endogenous Abs attached to the effector cell surface through FcγR binding). In this study, we demonstrate that the magnitude of NK cell–mediated ADCC response toward RBCs depends on a complex interplay between Ag, Ab glycosylation, target, and effector cell properties.

Materials and Methods

mAb production and glycoengineering

Expression vectors (pcDNA3.1) encoding human monoclonal IgG1 with specificity for Kell (more specifically: K Ag, referred to as K) (24), Rhesus D (RhD) (4, 25) or 2,4,6-trinitrophenol (TNP) (26) Ag were transfected into HEK 293 Freestyle cells using 293fectin (Invitrogen) or PEI MAX (Polysciences) (24–26). To produce hypofucosylated IgG1 Abs, 0.2 mM 2-deoxy-2-fluoro-*l*-fucose (Carbosynth) was added to the culture 1 h prior to transfection. After 5 d, the supernatant was harvested, filtered, and purified on an ÄKTAprime plus system (GE Healthcare Life Sciences) by affinity chromatography using a protein A HiTrap HP column (GE Healthcare Life Sciences), as previously described (4).

Cells

NK cells were obtained from heparinized blood of healthy donors, genotyped for *FCGR3A*-Val/Phe158 (or *FCGR3A*-Val/Phe176) polymorphism (rs396991), and selected to have two copies of the *FCGR3A* gene and no open reading frame for *FCGR2C* (27, 28). Genotyping was performed by multiplex ligation-dependent probe amplification as described previously (29). NK cells were freshly isolated the day prior to the ADCC assay from Ficoll-Plaque Plus (GE Healthcare Life Sciences) gradient-obtained PBMC fraction using anti-human CD56-coated MACS MicroBeads (Miltenyi Biotec) according to manufacturer's protocol. After isolation, NK cells were incubated overnight at 37°C and 5% CO_2 in IMDM (Life Technologies) supplemented with 10% (v/v) FCS at a density of 1–1.5 × 10^6 cells/ml.

RBCs were obtained from well-characterized donors expressing K Ag on the Kell glycoprotein or RhD at different levels: R2R2 (DcE/DcE; 15,800–33,300 RhD per cell), R1r (DCe/dce; 9900–14,600 RhD per cell) and weak D type 3 (DCe/dce; <100–10,000 RhD per cell) (30). Isolated RBCs were kindly provided by the Department of Erythrocyte Diagnostics, Sanquin. RBCs were treated with 0.5% bromelain (K1121; Sanquin) by adding bromelain 2:1 to packed cells and incubating for 10 min at 37°C. For neuraminidase treatment, 1 U/ml neuraminidase (Roche) was diluted in PBS and added 1:1 to packed cells, and cells were incubated for 20 min at 37°C. To facilitate TNP-lation of RBCs, packed cells were incubated with various concentrations (25–0.2 μM) of 2,4,6-trinitrobenzene sulfonic acid (Sigma-Aldrich) 1:1 diluted in Na_2HPO_4 buffer (pH 10) (4) and incubated at room temperature for 10 min. After treatment, RBCs were washed three times with PBS.

NK cell Ab elution

MACS-isolated NK cells were washed in RPMI 1640 medium without additives (Life Technologies) and centrifuged for 5 min at 700 × *g*. The cells were subsequently incubated in RPMI 1640 (pH 7.4) or HCl-acidified RPMI 1640 (pH 3.0) at 1 × 10^7 cells/ml for 5 min, after which the cells were spun down again (5 min, 700 × *g*). The supernatant was collected and diluted 1:1 with normal RPMI 1640 to neutralize the low pH. Cells were resuspended in PBS supplemented with 0.1% (v/v) BSA for further analysis with flow cytometry. The overnight elution step is described in the previous subsection. For plasma reconstitution of overnight-eluted NK cells, cells were incubated with their own undiluted or 100× diluted donor-specific plasma for 30 min at room temperature. Subsequently, these cells were washed twice in RPMI 1640 medium.

IgG ELISA

To determine concentrations of IgG from donor plasma and eluted from NK cells, IgG ELISA was performed as described previously with some adaptations (31). Ninety-six-well flat-bottom plates (Nunc MaxiSorp) were coated overnight at 4°C with 100 μl (1 μg/ml) mouse anti-human IgG (R10Z8E9; Abcam). Plates were blocked and subsequently incubated for 1 h with 100 μl sample 1:1 diluted in PBS supplemented with 0.05% (v/v) Tween 20. Next, plates were incubated with 100 μl (1 μg/ml) HRP-conjugated mouse anti-human IgG (clone MH16, PeliClass; Sanquin) for 1 h. Plates were washed three times with PBS 0.05% (v/v) Tween 20 in between each incubation step, and detection was performed with tetramethylbenzidine and stopped with 2 M H_2SO_4. Absorbance was measured at on a BioTek plate reader (BioTek), and sample IgG1 concentrations were calculated by interpolation using a defined IgG standard curve.

IgG glycosylation analysis

IgG Abs were purified from 1 μl serum and 100 μl NK cell eluates using CaptureSelect FcXL Affinity Matrix (Thermo Fisher Scientific) in a 96-well filter plate (Millipore MultiScreen) as described previously (32). Purified IgG molecules were eluted with 100 mM formic acid (Honeywell) into V-bottom plates and dried by vacuum centrifugation for 2.5 h at 60°C. IgG molecules were then dissolved in 50 mM ammonium bicarbonate (Sigma-Aldrich), and 200 ng sequencing grade modified trypsin (Promega) was added. After 17 h incubation samples were stored at −20°C until usage.

Purified glycopeptides from sera were diluted 50×, and the NK cell eluates were subjected in undiluted form to reverse phase nano–liquid chromatography-mass spectrometry analysis using an UltiMate 3000 RSLCnano system (Dionex/Thermo Fisher Scientific) coupled to a maXis HD Quadrupole Time-of-Flight Mass Spectrometer (Bruker Daltonics) equipped with a Nano-Booster (Bruker Daltonics) using acetonitrile-doped nebulizing gas (liquid chromatography-mass spectrometry grade; BioSolve). (Glyco-) peptides were trapped with 100% solvent A (0.1% formic acid in water) and separated on a gradient of water (solvent A) and 95% acetonitrile (solvent B) with 0.1% formic acid: 1% B 0–5 min, linear gradient to 27% B 5–20 min, washing at 70% B 21–23 min, and re-equilibration

at 1% B 24–58 min. In the current study, we focused on IgG1, without analyzing IgG3 because of its possible interference with IgG2 and IgG4 at the glycopeptide level (33). Mass spectrometry data were analyzed using Skyline software, and peptide MS1 trace quantification was judged reliable when retention times and mass accuracy matched an IgG standard digest and the experimental isotope envelop for each peptide matched the theoretical distribution. In addition, all traces were manually inspected and removed when they were close to noise or contained peptide/chemical interferences. The total level of glycan traits was calculated as described previously by Dekkers et al. (4).

ADCC assay

NK cell–mediated ADCC assays were performed as previously described, with some small adjustments (4). Briefly, overnight-incubated NK cells were centrifuged at 1700 rpm for 7 min and resuspended in fresh IMDM medium supplemented with 10% (v/v) FCS. RBC target cells (1×10^8) were labeled with 100 μCi ^{51}Cr (PerkinElmer) for 45 min at 37°C. After labeling, RBCs were washed twice with PBS, followed by resuspension in IMDM supplemented with 10% (v/v) FCS at a concentration of 4×10^5/ml. ^{51}Cr-labeled target cells were mixed with NK cells in an E:T ratio of 1:2 (0.5×10^5:1×10^5) in the presence of the specific Ab (anti-RhD/K/TNP, at indicated concentrations) and pelleted in 96-well V-bottom plates (Thermo Fisher Scientific). In the blocking experiment, NK cells were first incubated for 15 min with serially diluted anti-TNP Abs at 37°C and subsequently mixed with the anti-RhD Ab and target cells. After incubating the plates for 2 h at 37°C, the supernatant was collected, and radioactivity was measured in a Cobra II Gamma Counter (Packard BioScience). Background and maximal killing were determined by incubating target cells in IMDM only and IMDM medium containing 2.5% (v/v) saponin (Fluka; Sigma-Aldrich), respectively. Cell lysis percentages were eventually calculated by using the following formula:

$$\text{Lysed cells}(\%) = \left(\left(\text{cpm}_{\text{sample}} - \text{cpm}_{\text{background}}\right) / \left(\text{cpm}_{\text{maximal}} - \text{cpm}_{\text{background}}\right)\right) \times 100\%$$

All samples were measured in triplicate per experiment.

Flow cytometry

To determine RBC opsonization levels, anti-RhD/K/TNP Abs were titrated in PBS (at concentrations indicated in the figures and figure legends) and allowed to bind their specific Ag on the RBC membrane for 30 min at 4°C. After two washes, the cells (5×10^5) were incubated with PE-conjugated goat anti-human IgG1 F(ab′)$_2$ fragments (SouthernBiotech) for 30 min at 4°C. All dilutions, suspensions and washes were performed in PBS supplemented with 0.5% (v/v) BSA (Sigma-Aldrich).

Sambucus nigra agglutinin (Vector Laboratories) was conjugated to Dylight 405 using Dylight Conjugation Kit (Thermo Fisher Scientific) according to manufacturer's instructions and were used to determine sialic acid content on bromelain- and neuraminidase-treated RBCs (5×10^5). Glycophorin A (GPA) levels on bromelain- or neuraminidase-treated RBCs (5×10^5) were determined by staining with a primary mouse anti-human GPA IgG1 (Sanquin Reagentia), followed by a secondary allophycocyanin-conjugated goat anti-mouse IgG1 (Thermo Fisher Scientific) stain. Untreated RBCs were taken along as positive control.

After the final staining incubation, cells were washed twice. At least 10,000 events were measured on a FACSCanto II (BD Biosciences). For RBC sample gating, forward and side scatter were set on log scale, and the threshold was set on 200. The MACS-isolated NK cells were gated based on their characteristic forward and side scatter pattern to exclude other cell types from analysis.

Data analysis and statistics

Flow cytometry data were analyzed with FlowJo software version 10 (FlowJo) and BD FACSDiva software (BD Biosciences). Statistical analyses and nonlinear curve fitting (agonist versus response: variable slope, four parameters) were performed in GraphPad Prism software version 7.04 (GraphPad Software). The level of significance was set at $p \leq 0.05$ and determined using multiple, two-tailed paired or unpaired t tests, as indicated in figure legends.

Results

Opsonization degree of target cells depends on Ag density

We first assessed the influence of Ag density on the opsonization degree of target cells using two Abs targeting RBC blood group Ags (RhD and Kell) and one Ab targeting a randomly coupled TNP Ag. Coupling of TNP Ags to RBCs (TNP-lation) facilitated the analysis of a wide range of Ag densities. In addition, well-characterized RBC donors were selected expressing either the K Ag on the Kell glycoprotein (referred to as K; 3500–6100 Ags per RBC) or RhD at high (R2R2; 15,800–33,300), intermediate (R1r; 9900–14,600), or low (weak D; <100–10,000) levels (30). These specific RBCs were opsonized with a saturating concentration of a human mAb targeting the respective Ag (Supplemental Fig. 1). As expected, IgG opsonization of RBCs correlated with Ag density (Fig. 1A). A 30-fold difference in opsonization was observed between high (12.5 μM) and low (3.1 μM) TNP-lated RBCs as measured by geometric mean fluorescent intensity (gMFI) of 18,600 and 616, respectively, which was roughly consistent with the 32-fold lower degree of TNP-lation. Between R2R2 and weak D RBCs, a 25-fold difference in opsonization level was observed (gMFI of 28,287 and 1115, respectively). Opsonization of K$^+$ RBCs was in a similar range as opsonization of weak D RBCs, which is in line with the Ag densities described for these blood groups (30).

NK cell–mediated ADCC depends on the density of target Ag and IgG fucosylation status

Next we analyzed ADCC of the various Ag-dense target cells with NK effector cells from FcγRIIIa$^{\text{Val/Val158}}$ donors [two *FCGR3A*-Val158 gene copies and no open reading frame for *FCGR2C* (27, 28)]. In general, Ag density correlated with ADCC capacity of fucosylated and hypofucosylated Abs, where higher Ag density on the target cell led to higher ADCC responses (Fig. 1B). RBCs were consistently lysed more efficiently in the presence of hypofucosylated Abs compared with their fucosylated counterpart (Fig. 1B). Consistent with previous ADCC experiments with fucosylated anti-RhD Abs (4), negligible killing of R1r and weak D target cells was observed. However, a small ADCC response (~5%) was observed when RBC with high RhD Ag density (R2R2) were used as target cells, suggesting that one of the factors limiting ADCC with fucosylated anti-RhD Abs is the low RhD expression on RBCs. Low Ag density also appeared to limit NK cell–mediated ADCC of K Ag–expressing RBCs with fucosylated anti-K Abs (Fig. 1A, 1B).

Interestingly, RBCs with randomly coupled TNP triggered higher ADCC with fucosylated and hypofucosylated IgG1 compared with RhD-expressing R2R2 and R1r target cells under a similar level of opsonization (Fig. 1, Supplemental Fig. 2A, 2B). For example, NK cell–mediated ADCC of 6.3 μM TNP-lated RBCs was more efficient compared with the ADCC of R1r RBCs (fucosylated IgG1 $p < 0.0001$; hypofucosylated IgG1; $p = 0.0053$) (Fig. 1B). However, this difference in ADCC between comparable opsonization levels was lost at lower Ag densities (weak D versus 0.8 μM TNP-lated RBC, $p = 0.185$, $p = 0.952$) (Fig. 1B). Because of the differential functional response between anti-TNP and anti-RhD at higher opsonization levels (R2R2 and R1r RhD compared with equivalent anti-TNP opsonization), we hypothesized that this may be because of differential Ag position or mobility with respect to the plasma membrane. The negative surface charge (34, 35) of RBCs, resulting from a thick glycocalyx with sialic acid–containing glycans, inflicts repulsive forces toward other cells (ζ-potential) and normally prevents agglutination of RBCs (36, 37). Because TNP is randomly coupled, its distance from the RBC lipid membrane is most likely more variable compared with the natural Ags on Kell (globular extracellular domain) and RhD (multispanning membrane protein) which are known to be very close to the membrane (38, 39). Therefore, ADCC synapses involving anti-TNP may theoretically form more readily because (part of) the epitopes are more accessible, more mobile, and/or may

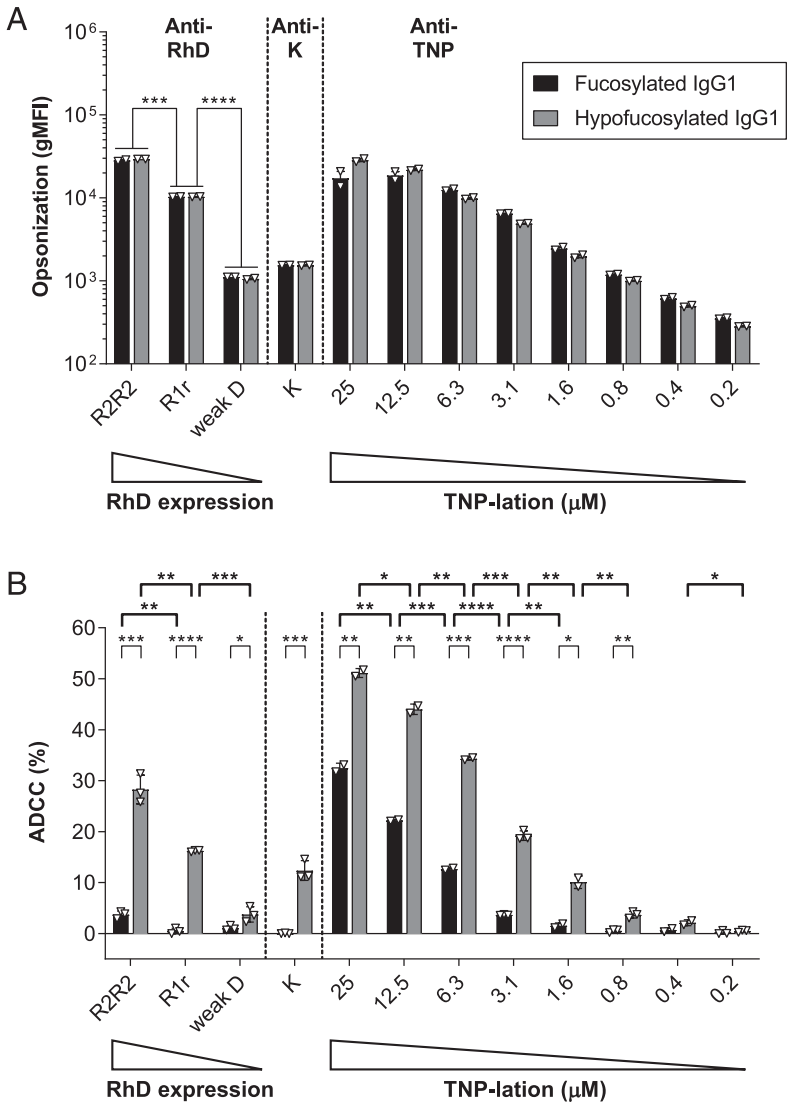

FIGURE 1. NK cell–mediated ADCC depends on Ag density. (**A**) Opsonization levels of RhD- and K Ag–expressing and TNP-lated RBCs with their specific fucosylated (black bars) or hypofucosylated (gray bars) monoclonal IgG1 (5 μg/ml). Data represent gMFI ± SEM values. (**B**) NK cell–mediated ADCC (percentage ± SEM) toward RBCs opsonized with fucosylated or hypofucosylated IgG1, as depicted in (A). NK cells were obtained from FcγRIIIa$^{Val/Val158}$ donors. In this figure, data from one experiment performed in duplicate or triplicate are plotted as a representative of three independent experiments. Individual data points are depicted as white triangles, with bar graphs indicating the mean. Significant differences were determined by two-tailed unpaired *t* test and are indicated with asterisks. *$p < 0.05$, **$p < 0.01$, ***$p < 0.001$, ****$p < 0.0001$.

encounter less repulsive forces compared with anti-RhD/anti-K synapses which require Ag–Ab interactions closer to the membrane.

RBC glycocalyx limits ADCC activity

To test the effect of the RBC glycocalyx on NK cell–mediated ADCC, RhD$^+$, K$^+$, and TNP-lated RBCs were treated with the protease bromelain, which digests the glycoproteins that make up the RBC glycocalyx by cleaving these preferentially after a lysine, alanine, or tyrosine residue (37). Overall, ADCC of RBCs was markedly enhanced when bromelain-treated RBCs were used (Fig. 2A). Most strikingly, bromelain treatment significantly increased the ADCC efficiency of R2R2 RBCs with fucosylated anti-RhD from 3.7 to 67.1% ($p = 0.0012$) and of R1r RBCs from 0.5 to 30.7% ($p = 0.0009$) (Fig. 2A, Supplemental Fig. 2A, 2B). At low Ag density (weak D and K), bromelain treatment enhanced ADCC with hypofucosylated Abs ($p = 0.0041$, $p = 0.0147$), which was not observed with the fucosylated counterpart ($p = 0.2294$, $p = 0.2534$) (Fig. 2A, Supplemental Fig. 2C). Overall, at similar opsonization levels, bromelain-induced fold differences were lower for ADCC with fucosylated anti-TNP Abs than with anti-RhD Abs (Fig. 2A, Supplemental Fig. 2A, 2B), suggesting that the glycocalyx more strongly limits ADCC for RhD than for TNP epitopes. In addition, this illustrates that removal of the glycoprotein layer enhances ADCC responses without increasing the opsonization level of RBCs.

Because bromelain cleaves all glycoproteins in the RBC membrane, including the highly abundant glycoprotein GPA (Supplemental Fig. 2D), both the removal of the physical barrier and the removal of negative surface charge (ζ-potential) of the RBC might explain the enhanced ADCC. To reduce the ζ-potential while retaining the physical barrier, RBCs were treated with the enzyme neuraminidase, which specifically cleaves of negatively charged α-2,6–linked sialic acids (Supplemental Fig. 2E). Neuraminidase treatment of RBCs enhanced ADCC capacity in a similar manner as bromelain treatment (Fig. 2B–F), suggesting that the negative ζ-potential of the glycocalyx rather than the physical barrier limits ADCC potency.

FcγRIIIa phenotype influences ADCC potency toward RBCs and depends on ζ-potential

To define the influence of the FcγRIIIa–Val/Phe158 polymorphism on ADCC activity, NK cells from 18 *FCGR3A*-genotyped healthy volunteers were tested in the ADCC setup with R2R2 RBCs. When untreated RBCs with high RhD expression (R2R2) were used as target cells, the FcγRIIIa phenotype (from low to high affinity: Phe/Phe158, Val/Phe158, and Val/Val158) did significantly affect NK cell–mediated ADCC, both with fucosylated and hypofucosylated anti-RhD IgG1 (Fig. 3). These changes were relatively small, which is consistent with previous findings (4, 8). However, ADCC of bromelain-treated R2R2 RBCs with a

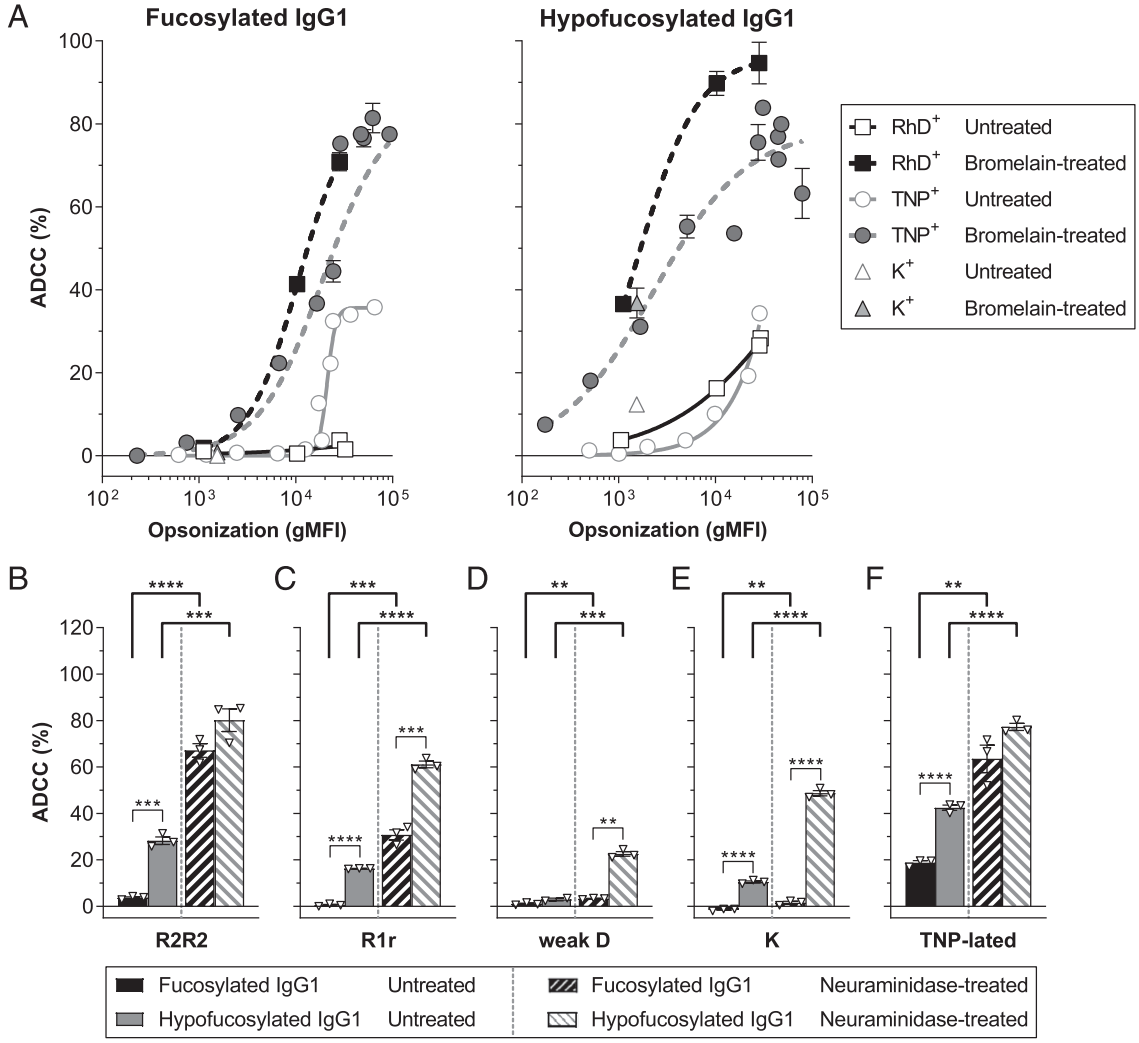

FIGURE 2. Sialic acid content of the RBC glycocalyx dampens ADCC by NK cells. (**A**) Correlation between ADCC (percentage ± SEM) and mean opsonization levels measured by gMFI by fucosylated (left panel) and hypofucosylated (right panel) IgG1 for untreated (open symbols) or bromelain-treated (filled symbols) TNP-lated (gray circles), RhD- (black squares), and K- (light gray triangles) expressing RBC targets. Curves (solid for untreated and dashed for bromelain-treated) represent nonlinear fitting. (**B**–**F**) (B) R2R2, (C) R1r, (D) weak D RhD-, (E) K-expressing, and (F) TNP-lated RBCs were treated with neuraminidase (striped bars) or not (solid bars) and subsequently used as target cells in the NK cell–mediated ADCC assay in the presence of fucosylated (black) or hypofucosylated (gray) IgG1 against the specific Ag. ADCC responses (percentage ± SEM). In this figure, one experiment performed in triplicate is depicted as a representative of three independent experiments. Individual data points are depicted as white triangles with bar graphs indicating the mean (B–F). NK cells were obtained from FcγRIIIa$^{Val/Val158}$ donors. Significant differences within groups between fucosylated and hypofucosylated were determined by two-tailed paired *t* test and between treatments by two-tailed unpaired *t* test and indicated with asterisks. Statistical comparisons between groups for fucosylated and hypofucosylated IgG1 are depicted in bold. $^{**}p < 0.01$, $^{***}p < 0.001$, $^{****}p < 0.0001$

fucosylated anti-RhD Ab was highly dependent on the FcγRIIIa phenotype of the NK cell donor (Fig. 3). Under these conditions (bromelain-treated R2R2 and fucosylated anti-RhD IgG1), the ADCC capacity with Val/Phe158- or Val/Val158-expressing effector cells was almost 3-fold higher compared with Phe/Phe158-expressing NK cells (Phe/Phe158 mean 28.2% and Val/Val158 76.9%, $p = 0.0006$; Phe/Phe158 28.2% and Val/Phe158 78.4%, $p < 0.0001$). This was also observed for intermediate (R1r) and low (weak D) RhD-expressing target cells after bromelain treatment (Supplemental Fig. 3). In general, the influence of the FcγRIIIa phenotype of the NK cell was absent or less prominent using hypofucosylated anti-RhD Abs (Fig. 3, Supplemental Fig. 3).

Quantity and fucosylation status of cytophilic Abs determine the capacity to block ADCC responses by specific Abs

The large amount of aspecific endogenous/cytophilic Abs present in vivo competes for binding to FcγRIIIa on NK cells and potentially interferes with ADCC responses. To study this, we first determined the blocking capacity of fucosylated and hypofucosylated anti-TNP Abs, which may compete for FcγR binding, in the anti-RhD ADCC assay. In line with the higher affinity for FcγRIIIa, hypofucosylated anti-TNP Abs blocked ADCC of RBCs by fucosylated anti-RhD IgG1 more efficiently compared with the fucosylated counterpart (Fig. 4A).

We confirmed the presence of cytophilic IgG on freshly isolated NK cells, where the quantity was slightly higher on NK cells from FcγRIIIa$^{Val/Val158}$ donors (Fig. 4B, 4C), which is consistent with previous observations (40). To capture and study these cytophilic Abs, acid elution (5 min at pH 3.0) was performed, which resulted in the depletion of Abs from the NK cells (Fig. 4B, Supplemental Fig. 4A). The fucosylation degree of these cytophilic Abs was substantially lower than found in plasma (Fig. 4D, left panel; Supplemental Fig. 4B, left panel), consistent with higher affinity of hypofucosylated IgG1 for FcγRIIIa (4, 8, 16–18), which will

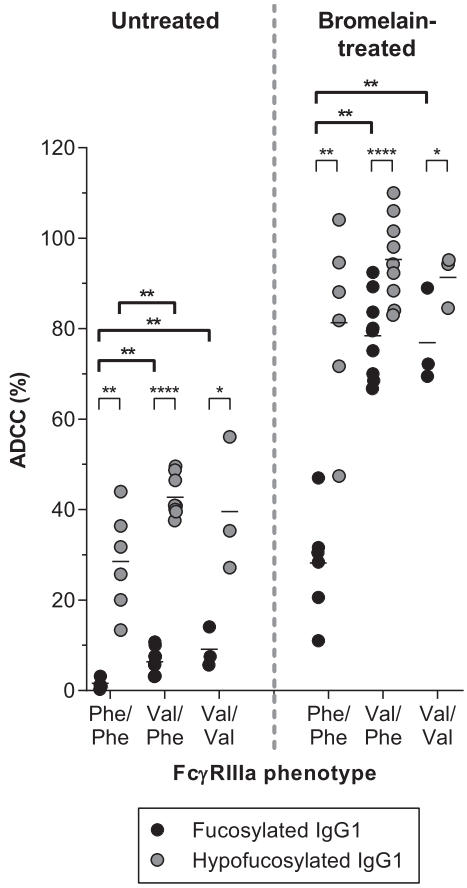

FIGURE 3. FcγRIIIa–Val/Phe158 polymorphism influences ADCC by fucosylated IgG1. Scatter dot plot showing mean ADCC responses (percentage) of NK cells from 18 different *FCGR3A*-genotyped donors (specified for FcγRIIIa phenotypes: Phe/Phe158, Val/Phe158, Val/Val158) toward untreated (left of dotted line) or bromelain-treated (right of dotted line) RhD-expressing RBCs (R2R2) in the presence of fucosylated (black dots) or hypofucosylated (gray dots) anti-RhD IgG1 (5 μg/ml). For each donor, the mean value of an experiment performed in triplicate is plotted. Statistically significant differences between ADCC conditions using the same NK cell donor were determined by two-tailed paired *t* test. Statistically significant differences for fucosylated or hypofucosylated IgG1 between NK cells of different phenotype are depicted in bold and were determined by two-tailed unpaired *t* test. Significant differences are indicated with asterisks. $*p < 0.05$, $**p < 0.01$, $****p < 0.0001$.

thus remain longer on NK cells during isolation procedures. Next, we assessed whether these NK cell–bound cytophilic IgG influence ADCC responses as we observed for anti-TNP IgG (Fig. 4A). Results show that the remaining FcγRIIIa-bound cytophilic Abs present on freshly isolated NK cells did not inhibit or only subtly inhibit ADCC activity in our in vitro assay compared with NK cells that were IgG depleted by overnight incubation (20 h at 37°C) to retain viability and functionality (Fig. 4E).

To mimic in vivo situations, overnight-eluted NK cells were reconstituted with their own donor-specific plasma. The amount of NK cell–bound IgG was ∼10-fold higher compared with freshly isolated NK cells (Fig. 4C), and subsequent acid elution of these plasma-reconstituted NK cells revealed that the fucosylation degree was slightly lower compared with plasma IgG (Fig. 4D, right panel; Supplemental Fig. 4B, right panel). The plasma reconstitution step appeared to decrease the ADCC response induced by fucosylated anti-RhD IgG1, but not by hypofucosylated anti-RhD (Fig. 4E). When a 100× diluted plasma fraction was used to reconstitute NK cells, the ADCC response was not decreased, indicating that a high occupancy of FcγRIIIa on NK cells is necessary to have blocking effect on ADCC via fucosylated anti-RhD IgG1 (Fig. 4E). In conclusion, the cytophilic Abs on isolated NK cells showed lower fucosylation but did not influence in vitro ADCC responses. However, cytophilic Abs are potentially blocking ADCC responses in vivo, depending on the Ab concentration and fucosylation status. Therefore, cytophilic IgG could be considered as another parameter affecting NK cell–mediated ADCC in addition to the other parameters identified in this study (Fig. 5).

Discussion

ADCC is one of the most important effector mechanism of tumor-targeting therapeutic Abs. In this study, we determined the contribution of five parameters to the induction of NK cell–mediated ADCC in vitro. These are visualized in Fig. 5, which shows the complete spectrum, starting from the least potent ADCC response (low Ag density, fucosylated IgG, low-affinity FcγRIIIa-Phe/Phe158 phenotype, with glycocalyx intact) to the most potent ADCC response (high Ag density, hypofucosylated IgG, high-affinity FcγRIIIa–Val/Val158 phenotype, in the absence of target cell glycocalyx). We found that the magnitude of the ADCC response highly depends on Ag density for both fucosylated and hypofucosylated Abs. On the side of the effector cells, NK cells expressing the FcγRIIIa–Val158 polymorphic variant inflict higher target cell lysis. Interestingly, we identified the negative charge of the target cell glycocalyx (ζ-potential) as an important limiting factor for ADCC capacity. All of these factors determine potency of Abs and are therefore likely important for translation to their in vivo capacity.

One obvious parameter that we studied was the Ag density of the target cell. Our data are consistent with previous observations, in which Ag density on the target cell correlated with the potency of anti–HER2/*neu* Abs to trigger a proper ADCC response toward HER2/*neu*–positive tumor cells (41, 42). A higher Ag density on RBCs was required for RhD compared with TNP to achieve a similarly strong ADCC response, indicating that other factors besides Ag density are influencing ADCC potency, including Ag mobility, flexibility, accessibility, and the stoichiometry of the Ab–Ag and/or Ab affinity. We only found a subtle ADCC response with fucosylated anti-RhD using RBCs with natural but high RhD expression levels (R2R2), whereas no ADCC was observed when intermediate- (R1r) and low-expressing (weak D) target cells were used. In previous studies, we did not select target RBCs based on RhD expression levels and, therefore, most likely used the most common phenotypes R1R1 (prevalence: 41.0–43.8%) and R1r (25.5–32.2%) in the ADCC assays rather than the less-prevailing R2R2 (0.7–4.7%), which explains why we previously did not observe ADCC responses toward RBCs using fucosylated anti-RhD IgG1 (4, 8). Hypofucosylation of anti-TNP, anti-K, or anti-RhD IgG1 resulted in potentiation of the ADCC response toward the same target cell (1, 4, 8), which was also observed in other studies (20) and in this study for all Ag-expressing RBCs, emphasizing the importance of Ab fucosylation status for ADCC.

In this study, the ADCC potential with fucosylated anti-RhD IgG1 differed significantly between NK cells from FcγRIIIa$^{Val/Val158}$/FcγRIIIa$^{Val/Phe158}$ and FcγRIIIa$^{Phe/Phe158}$ donors, which is consistent with the 2–5-fold higher affinity of IgG1 for the FcγRIIIa–Val158 variant. This difference is in agreement with other studies showing FcγRIIIa–Val/Phe158 polymorphism-dependent ADCC kinetics (43, 44). However, the extent of the differential ADCC between the FcγRIIIa phenotypes was also dependent on the glycocalyx and whether the Abs were fucosylated or not. This likely explains why the difference in NK cell–mediated

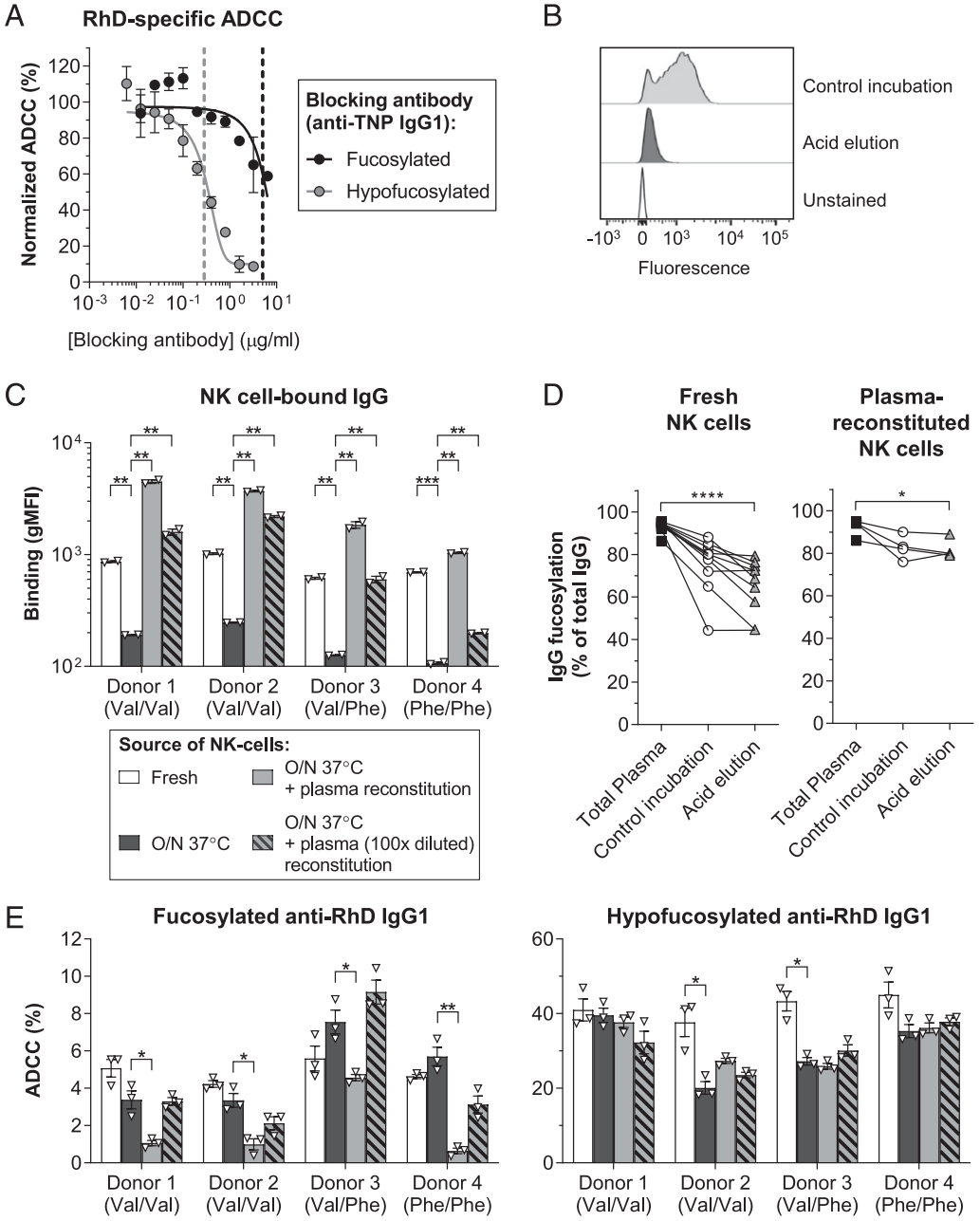

FIGURE 4. Cytophilic Ab fucosylation status and their blocking capacity in ADCC responses. (**A**) Concentration-dependent blocking of fucosylated anti-RhD IgG1- (0.2 μg/ml) specific ADCC response (normalized percentage ± SEM) by fucosylated (black) or hypofucosylated (gray) aspecific anti-TNP IgG1. A control condition without blocking Abs was used to normalize the ADCC values (control set at 100%). Calculated IC_{50} are indicated by vertical dashed lines for blocking by fucosylated (black) or hypofucosylated (gray) anti-TNP IgG1. One experiment performed in triplicate is depicted as a representative of three independent experiments. (**B**) Illustrative flow cytometry histograms showing the presence of cytophilic IgG on freshly isolated NK cells after control (pH 7.4) (light gray) or acid (pH 3.0) (dark gray) elution. Unstained cells (white) were included for control purposes. Cytophilic IgG on NK cells was detected by goat anti-human IgG $F(ab')_2$ fragments. (**C**) Presence (as measured by gMFI ± SEM) of human IgG on fresh (white) or 37°C overnight (O/N)–eluted NK cells that were subsequently reconstituted (or not, dark gray) with their own undiluted (light gray) or original magnification ×100–diluted (light gray, striped) donor-specific plasma. NK cells were isolated from four different donors, and their corresponding FcγRIIIa phenotype is included in the figure. One experiment performed in duplicate is depicted as a representative of three independent experiments. Individual data points are depicted as white triangles with bar graphs indicating the mean. Significant differences have been determined by multiple *t* test with Holm–Sidak correction. $^{**}p < 0.01$, $^{***}p < 0.001$. (**D**) Asn297 fucosylation (percentage) of IgG eluted from freshly isolated NK cells (left panel, 10 donors) and from O/N-eluted NK cells that have been reconstituted with their own donor-specific plasma prior to acid elution (right panel, four donors). Fucosylation degrees have been determined by mass spectrometry. IgG fucosylation was analyzed from total plasma (black squares) and from NK cells after control (pH 7.4) (white circles) and acid (pH 3.0) (light gray triangles) elution. Samples from the same donor are connected by a line. See Supplemental Fig. 4B for additional glycosylation traits. Statistical differences between fucosylation levels of total plasma and acid-eluted IgG were determined by two-tailed paired *t* test and significant differences are indicated with asterisks. $^{*}p < 0.05$, $^{****}p < 0.0001$. (**E**) ADCC responses (percentage ± SEM) of NK cells [various treatments as in (C) toward R2R2 cells with fucosylated (left panel) and hypofucosylated (right panel) anti-RhD IgG1 (5 μg/ml)]. One experiment performed in triplicate is depicted as a representative of three independent experiments. Individual data points are depicted as white triangles with bar graphs indicating the mean. Significant differences have been determined by multiple *t* test with Holm–Sidak correction. $^{*}p < 0.05$, $^{**}p < 0.01$.

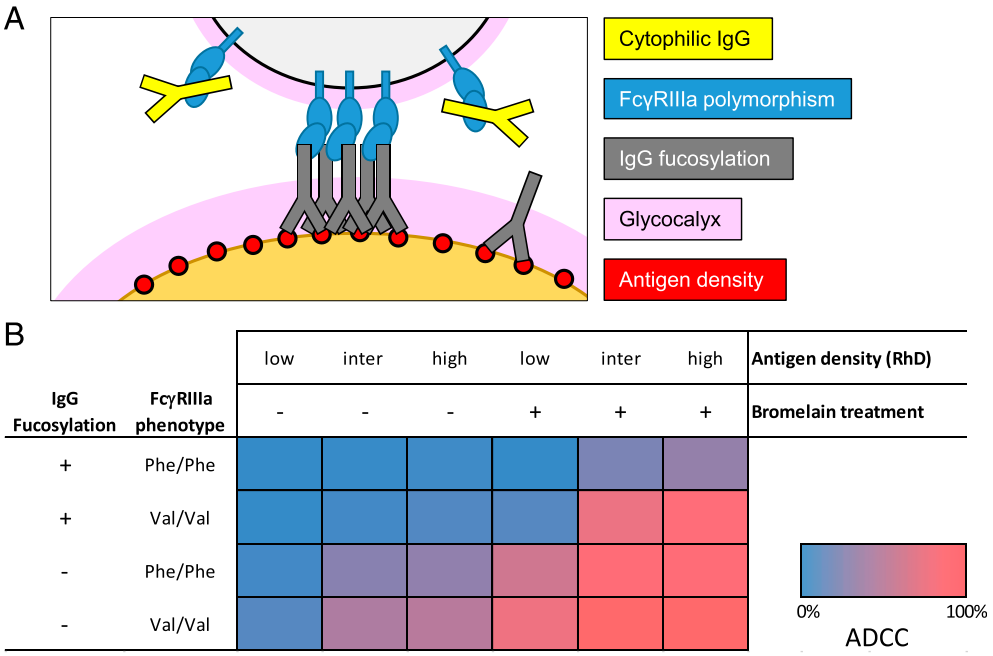

FIGURE 5. Parameters involved in NK cell–mediated ADCC. (**A**) Schematic representation of the immunological synapse between effector (gray) and IgG-opsonized target cells (orange) via Ab-FcγRIIIa (blue) interactions. Parameters depicted in this figure are Ag (red circles) density, ζ-potential/glycocalyx (pink, with thickness indicating the magnitude of negative surface charge), and IgG1 (dark gray) fucosylation status and cytophilic Abs (yellow). (**B**) Overview giving the spectrum of parameters (depicted in A) determining ADCC magnitude with anti-RhD IgG1. ADCC percentages are derived from the results depicted in Fig. 3 and Supplemental Fig. 3. To illustrate ADCC magnitude, percentages are color coded from 0% killing (red) to 100% killing (blue).

ADCC activity between FcγRIIIa$^{Val/Val158}$, FcγRIIIa$^{Val/Phe158}$, or FcγRIIIa$^{Phe/Phe158}$ donors was less pronounced using hypofucosylated anti-RhD IgG1 (4). An additional aspect not investigated in this study that can influence NK cell–mediated ADCC is *FCGR3A* gene copy number variation, which has been demonstrated to correlate with receptor expression on the NK cell surface and target cell lysis (29, 45).

To study the influence of the target cell membrane glycoprotein layer on ADCC, the RBC glycocalyx was trimmed using bromelain. In general, this treatment enhanced ADCC responses to RBC target cells. At the saturating IgG1 concentration used in these assays, opsonization levels were similar for bromelain-treated and untreated RBCs, suggesting that the observed ADCC differences were the result of the glycocalyx removal itself rather than increased Ag accessibility. When we specifically removed the negatively charged sugar moieties (sialic acid) from the glycocalyx, a similar increase in ADCC responses was seen as was seen for bromelain treatment, indicating that the repulsive force resulting from the ζ-potential is limiting ADCC and not the physical barrier of the glycocalyx. An alternative explanation for the increase in ADCC upon removal of sialic acid on the side of the target cell might be the recognition of sialic acid on the RBC via sialic acid–binding Ig-type lectin (SIGLEC) receptors on the NK cells. SIGLEC receptors 7 and 9 are inhibitory receptors on the NK cell that have been shown to limit ADCC when recognizing sialic acid on tumor target cells (46). If so, then it is also important to realize that MHC class I–related ligands become more available after target desialylation and cause increased degranulation of the NK cells via triggering of the NK group 2D (NKG2D) activating receptor (47). Interestingly, glycan composition of cancer cells is often changed, including altered sialic acid composition and increased levels on tumor cells, which appeared to correlate with disease severity (48). However, bromelain treatment of target cells, which, like neuraminidase treatment, increased ADCC magnitude, did not reduce the apparent sialic acid content exposed on the RBC surface (Supplemental Fig. 2E), suggesting that altered SIGLEC and NKG2D triggering cannot solely explain the observed enhancement of ADCC responses. The subtle increase of *S. nigra* agglutinin binding to target cells after bromelain treatment might be explained by the cleavage of glycoproteins, potentially resulting in simultaneous enhanced exposure of normally cryptic glycolipids. Further studies are necessary to determine the mechanism(s) underlying the glycocalyx-induced ADCC effects.

In addition to all the parameters on both the target cell and effector cell side that affect ADCC, the presence of cytophilic Abs was also found to influence ADCC capacity. In agreement with our findings, Patel et al. (49) also observed very recently a significantly lowered core fucosylation in cytophilic IgG bound to NK cell surface, also presumably to FcγRIIIa, compared with serum IgG. In our in vitro assays, however, cytophilic Abs did not affect ADCC because we used overnight-incubated NK cells that caused dissociation of cytophilic Abs. Plasma reconstitution of these NK cells, however, did decrease specific ADCC responses by fucosylated IgG1, which could not be observed for hypofucosylated IgG1, indicating that, under in vivo conditions, cytophilic IgG have the capacity to modulate ADCC responses. Depending on the location of the ADCC response, the amount of cytophilic Abs is likely to be different, which could to a certain degree determine the competition for FcγRIIIa and the potential blocking effect.

In this study, we assessed all parameters influencing the capacity of NK cells to induce target cell lysis. These parameters are also likely to be involved in other NK cell Ab-dependent functions, such as Ab-dependent NK cell activation, and it would therefore be interesting to include the quantification of IFN-γ and chemokine C-C motif ligand 4 (CCL4) secretion and the expression of degranulation marker CD107a in future studies (50).

We conclude that Ag density, FcγRIIIa polymorphism, and the target cell glycocalyx are important and independent limiting factors influencing ADCC of RBCs by NK cells, which can partly be overcome by using hypofucosylated IgG.

Acknowledgments

We thank all volunteers that provided blood for research purposes.

Disclosures

The authors have no financial conflicts of interest.

References

1. Kapur, R., L. Della Valle, M. Sonneveld, A. Hipgrave Ederveen, R. Visser, P. Ligthart, M. de Haas, M. Wuhrer, C. E. van der Schoot, and G. Vidarsson. 2014. Low anti-RhD IgG-Fc-fucosylation in pregnancy: a new variable predicting severity in haemolytic disease of the fetus and newborn. *Br. J. Haematol.* 166: 936–945.
2. Sonneveld, M. E., J. Koelewijn, M. de Haas, J. Admiraal, R. Plomp, C. A. M. Koeleman, A. L. Hipgrave Ederveen, P. Ligthart, M. Wuhrer, C. E. van der Schoot, and G. Vidarsson. 2017. Antigen specificity determines anti-red blood cell IgG-Fc alloantibody glycosylation and thereby severity of haemolytic disease of the fetus and newborn. *Br. J. Haematol.* 176: 651–660.
3. Wang, X., M. Mathieu, and R. J. Brezski. 2018. IgG Fc engineering to modulate antibody effector functions. *Protein Cell* 9: 63–73.
4. Dekkers, G., L. Treffers, R. Plomp, A. E. H. Bentlage, M. de Boer, C. A. M. Koeleman, S. N. Lissenberg-Thunnissen, R. Visser, M. Brouwer, J. Y. Mok, et al. 2017. Decoding the human immunoglobulin G-glycan repertoire reveals a spectrum of Fc-receptor- and complement-mediated-effector activities. *Front. Immunol.* 8: 877.
5. Peschke, B., C. W. Keller, P. Weber, I. Quast, and J. D. Lünemann. 2017. Fc-galactosylation of human immunoglobulin gamma isotypes improves C1q binding and enhances complement-dependent cytotoxicity. *Front. Immunol.* 8: 646.
6. Subedi, G. P., and A. W. Barb. 2015. The structural role of antibody N-glycosylation in receptor interactions. *Structure* 23: 1573–1583.
7. Ferrara, C., S. Grau, C. Jäger, P. Sondermann, P. Brünker, I. Waldhauer, M. Hennig, A. Ruf, A. C. Rufer, M. Stihle, et al. 2011. Unique carbohydrate-carbohydrate interactions are required for high affinity binding between FcgammaRIII and antibodies lacking core fucose. *Proc. Natl. Acad. Sci. USA* 108: 12669–12674.
8. Bruggeman, C. W., G. Dekkers, A. E. H. Bentlage, L. W. Treffers, S. Q. Nagelkerke, S. Lissenberg-Thunnissen, C. A. M. Koeleman, M. Wuhrer, T. K. van den Berg, T. Rispens, et al. 2017. Enhanced effector functions due to antibody defucosylation depend on the effector cell Fcγ receptor profile. *J. Immunol.* 199: 204–211.
9. Quast, I., C. W. Keller, M. A. Maurer, J. P. Giddens, B. Tackenberg, L.-X. Wang, C. Münz, F. Nimmerjahn, M. C. Dalakas, and J. D. Lünemann. 2015. Sialylation of IgG Fc domain impairs complement-dependent cytotoxicity. *J. Clin. Invest.* 125: 4160–4170.
10. Bruggeman, C. W., G. Dekkers, R. Visser, N. W. M. Goes, T. K. van den Berg, T. Rispens, G. Vidarsson, and T. W. Kuijpers. 2018. IgG glyco-engineering to improve IVIg potency. *Front. Immunol.* 9: 2442.
11. Kapur, R., I. Kustiawan, A. Vestrheim, C. A. M. Koeleman, R. Visser, H. K. Einarsdottir, L. Porcelijn, D. Jackson, B. Kumpel, A. M. Deelder, et al. 2014. A prominent lack of IgG1-Fc fucosylation of platelet alloantibodies in pregnancy. *Blood* 123: 471–480.
12. Wuhrer, M., L. Porcelijn, R. Kapur, C. A. M. Koeleman, A. Deelder, M. de Haas, and G. Vidarsson. 2009. Regulated glycosylation patterns of IgG during alloimmune responses against human platelet antigens. *J. Proteome Res.* 8: 450–456.
13. Wang, T. T., J. Sewatanon, M. J. Memoli, J. Wrammert, S. Bournazos, S. K. Bhaumik, B. A. Pinsky, K. Chokephaibulkit, N. Onlamoon, K. Pattanapanyasat, et al. 2017. IgG antibodies to dengue enhanced for FcγRIIIA binding determine disease severity. *Science* 355: 395–398.
14. Ackerman, M. E., M. Crispin, X. Yu, K. Baruah, A. W. Boesch, D. J. Harvey, A.-S. Dugast, E. L. Heizen, A. Ercan, I. Choi, et al. 2013. Natural variation in Fc glycosylation of HIV-specific antibodies impacts antiviral activity. *J. Clin. Invest.* 123: 2183–2192.
15. Baković, M. P., M. H. J. Selman, M. Hoffmann, I. Rudan, H. Campbell, A. M. Deelder, G. Lauc, and M. Wuhrer. 2013. High-throughput IgG Fc N-glycosylation profiling by mass spectrometry of glycopeptides. *J. Proteome Res.* 12: 821–831.
16. Chung, S., Y. L. Lin, C. Reed, C. Ng, Z. J. Cheng, F. Malavasi, J. Yang, V. Quarmby, and A. Song. 2014. Characterization of in vitro antibody-dependent cell-mediated cytotoxicity activity of therapeutic antibodies - impact of effector cells. *J. Immunol. Methods* 407: 63–75.
17. Falconer, D. J., G. P. Subedi, A. M. Marcella, and A. W. Barb. 2018. Antibody fucosylation lowers the FcγRIIIa/CD16a affinity by limiting the conformations sampled by the N162-glycan. *ACS Chem. Biol.* 13: 2179–2189.
18. Subedi, G. P., and A. W. Barb. 2016. The immunoglobulin G1 N-glycan composition affects binding to each low affinity Fc γ receptor. *MAbs* 8: 1512–1524.
19. Reichert, J. M. 2016. Antibodies to watch in 2016. *MAbs* 8: 197–204.
20. Suzuki, E., R. Niwa, S. Saji, M. Muta, M. Hirose, S. Iida, Y. Shiotsu, M. Satoh, K. Shitara, M. Kondo, and M. Toi. 2007. A nonfucosylated anti-HER2 antibody augments antibody-dependent cellular cytotoxicity in breast cancer patients. *Clin. Cancer Res.* 13: 1875–1882.
21. Sibéril, S., C. de Romeuf, N. Bihoreau, N. Fernandez, J.-L. Meterreau, A. Regenman, E. Nony, C. Gaucher, A. Glacet, S. Jorieux, et al. 2006. Selection of a human anti-RhD monoclonal antibody for therapeutic use: impact of IgG glycosylation on activating and inhibitory Fc γ R functions. *Clin. Immunol.* 118: 170–179.
22. Li, H., N. Sethuraman, T. A. Stadheim, D. Zha, B. Prinz, N. Ballew, P. Bobrowicz, B.-K. Choi, W. J. Cook, M. Cukan, et al. 2006. Optimization of humanized IgGs in glycoengineered *Pichia* pastoris. *Nat. Biotechnol.* 24: 210–215.
23. Bruhns, P., B. Iannascoli, P. England, D. A. Mancardi, N. Fernandez, S. Jorieux, and M. Daëron. 2009. Specificity and affinity of human Fcgamma receptors and their polymorphic variants for human IgG subclasses. *Blood* 113: 3716–3725.
24. Howie, H. L., M. Delaney, X. Wang, L. S. Er, G. Vidarsson, T. C. Stegmann, L. Kapp, J. N. Lebedev, Y. Wu, J. P. AuBuchon, and J. C. Zimring. 2016. Serological blind spots for variants of human IgG3 and IgG4 by a commonly used anti-immunoglobulin reagent. *Transfusion* 56: 2953–2962.
25. Dekkers, G., A. E. H. Bentlage, T. C. Stegmann, H. L. Howie, S. Lissenberg-Thunnissen, J. Zimring, T. Rispens, and G. Vidarsson. 2017. Affinity of human IgG subclasses to mouse Fc gamma receptors. *MAbs* 9: 767–773.
26. Kruijsen, D., H. K. Einarsdottir, M. A. Schijf, F. E. Coenjaerts, E. C. van der Schoot, G. Vidarsson, and G. M. van Bleek. 2013. Intranasal administration of antibody-bound respiratory syncytial virus particles efficiently primes virus-specific immune responses in mice. *J. Virol.* 87: 7550–7557.
27. van der Heijden, J., W. B. Breunis, J. Geissler, M. de Boer, T. K. van den Berg, and T. W. Kuijpers. 2012. Phenotypic variation in IgG receptors by nonclassical FCGR2C alleles. *J. Immunol.* 188: 1318–1324.
28. Breunis, W. B., E. van Mirre, M. Bruin, J. Geissler, M. de Boer, M. Peters, D. Roos, M. de Haas, H. R. Koene, and T. W. Kuijpers. 2008. Copy number variation of the activating FCGR2C gene predisposes to idiopathic thrombocytopenic purpura. *Blood* 111: 1029–1038.
29. Nagelkerke, S. Q., C. E. Tacke, W. B. Breunis, M. W. T. Tanck, J. Geissler, E. Png, L. T. Hoang, J. van der Heijden, A. N. M. Naim, R. S. M. Yeung, et al. 2019. Extensive ethnic variation and linkage disequilibrium at the *FCGR2/3* locus: different genetic associations revealed in Kawasaki disease. *Front. Immunol.* DOI: 10.3389/fimmu.2019.00185.
30. Reid, M. E., and C. Lomas-Francis. 2004. *The Blood Group Antigen FactsBook.* Elsevier, New York, p. 109–264.
31. Kapur, R., L. Della Valle, O. J. H. M. Verhagen, A. Hipgrave Ederveen, P. Ligthart, M. de Haas, B. Kumpel, M. Wuhrer, C. E. van der Schoot, and G. Vidarsson. 2015. Prophylactic anti-D preparations display variable decreases in Fc-fucosylation of anti-D. *Transfusion* 55: 553–562.
32. Falck, D., B. C. Jansen, N. de Haan, and M. Wuhrer. 2017. High-throughput analysis of IgG Fc glycopeptides by LC-MS. *Methods Mol. Biol.* 1503: 31–47.
33. Einarsdottir, H. K., M. H. J. Selman, R. Kapur, S. Scherjon, C. A. M. Koeleman, A. M. Deelder, C. E. van der Schoot, G. Vidarsson, and M. Wuhrer. 2013. Comparison of the Fc glycosylation of fetal and maternal immunoglobulin G. *Glycoconj. J.* 30: 147–157.
34. Omi, T., E. Kajii, and S. Ikemoto. 1994. The electrokinetic behavior of red blood cells from a patient with Tn syndrome by Doppler electrophoretic light scattering analysis. *Tohoku J. Exp. Med.* 174: 369–377.
35. Bondar, O. V., D. V. Saifullina, I. I. Shakhmaeva, I. I. Mavlyutova, and T. I. Abdullin. 2012. Monitoring of the zeta potential of human cells upon reduction in their viability and interaction with polymers. *Acta Naturae* 4: 78–81.
36. Eylar, E. H., M. A. Madoff, O. V. Brody, and J. L. Oncley. 1962. The contribution of sialic acid to the surface charge of the erythrocyte. *J. Biol. Chem.* 237: 1992–2000.
37. Fernandes, H. P., C. L. Cesar, and M. L. Barjas-Castro. 2011. Electrical properties of the red blood cell membrane and immunohematological investigation. *Rev. Bras. Hematol. Hemoter.* 33: 297–301.
38. Gruswitz, F., S. Chaudhary, J. D. Ho, A. Schlessinger, B. Pezeshki, C.-M. Ho, A. Sali, C. M. Westhoff, and R. M. Stroud. 2010. Function of human Rh based on structure of RhCG at 2.1 A. *Proc. Natl. Acad. Sci. USA* 107: 9638–9643.
39. Van Kim, C. L., Y. Colin, and J.-P. Cartron. 2006. Rh proteins: key structural and functional components of the red cell membrane. *Blood Rev.* 20: 93–110.
40. Koene, H. R., M. Kleijer, J. Algra, D. Roos, A. E. von dem Borne, and M. de Haas. 1997. Fc gammaRIIIa-158V/F polymorphism influences the binding of IgG by natural killer cell Fc gammaRIIIa, independently of the Fc gammaRIIIa-48L/R/H phenotype. *Blood* 90: 1109–1114.
41. Tang, Y., J. Lou, R. K. Alpaugh, M. K. Robinson, J. D. Marks, and L. M. Weiner. 2007. Regulation of antibody-dependent cellular cytotoxicity by IgG intrinsic and apparent affinity for target antigen. *J. Immunol.* 179: 2815–2823.
42. Velders, M. P., C. M. van Rhijn, E. Oskam, G. J. Fleuren, S. O. Warnaar, and S. V. Litvinov. 1998. The impact of antigen density and antibody affinity on antibody-dependent cellular cytotoxicity: relevance for immunotherapy of carcinomas. *Br. J. Cancer* 78: 478–483.
43. Jain, A., B. Poonia, E. C. So, R. Vyzasatya, E. E. Burch, H. S. Olsen, E. Y. Mérigeon, D. S. Block, X. Zhang, D. H. Schulze, et al. 2013. Tumour antigen targeted monoclonal antibodies incorporating a novel multimerisation domain significantly enhance antibody dependent cellular cytotoxicity against colon cancer. *Eur. J. Cancer* 49: 3344–3352.
44. Moroi, R., K. Endo, Y. Kinouchi, H. Shiga, Y. Kakuta, M. Kuroha, Y. Kanazawa, Y. Shimodaira, T. Horiuchi, S. Takahashi, and T. Shimosegawa. 2013. FCGR3A-158 polymorphism influences the biological response to infliximab in Crohn's disease through affecting the ADCC activity. [Published erratum appears in 2015 Immuno*genetics* 67: 545.] *Immunogenetics* 65: 265–271.
45. Breunis, W. B., E. van Mirre, J. Geissler, N. Laddach, G. Wolbink, E. van der Schoot, M. de Haas, M. de Boer, D. Roos, and T. W. Kuijpers. 2009. Copy number variation at the *FCGR* locus includes *FCGR3A, FCGR2C* and *FCGR3B* but not *FCGR2A* and *FCGR2B. Hum. Mutat.* 30: E640–E650.

46. Hudak, J. E., S. M. Canham, and C. R. Bertozzi. 2014. Glycocalyx engineering reveals a Siglec-based mechanism for NK cell immunoevasion. *Nat. Chem. Biol.* 10: 69–75.
47. Xiao, H., E. C. Woods, P. Vukojicic, and C. R. Bertozzi. 2016. Precision glycocalyx editing as a strategy for cancer immunotherapy. *Proc. Natl. Acad. Sci. USA* 113: 10304–10309.
48. Vajaria, B. N., K. R. Patel, R. Begum, and P. S. Patel. 2016. Sialylation: an avenue to target cancer cells. *Pathol. Oncol. Res.* 22: 443–447.
49. Patel, K. R., J. D. Nott, and A. W. Barb. 2019. Primary human natural killer cells retain proinflammatory IgG1 at the cell surface and express CD16a glycoforms with donor-dependent variability. *Mol. Cell. Proteomics*. DOI: 10.1074/mcp.RA119.001607.
50. Bernard, N. F., Z. Kiani, A. Tremblay-McLean, S. A. Kant, C. E. Leeks, and F. P. Dupuy. 2017. Natural killer (NK) cell education differentially influences HIV antibody-dependent NK cell activation and antibody-dependent cellular cytotoxicity. *Front. Immunol.* 8: 1033.